Colloid Polym Sci 275:1093–1107 (1997)

LEADING CONTRIBUTION

K. Nishinari

Rheological and DSC study of sol–gel transition in aqueous dispersions of industrially important polymers and colloids

Received: 17 June 1997
Accepted: 28 August 1997

Prof. Katsuyoshi Nishinari (✉)
Department of Food and Nutrition
Faculty of Human Life Science
Osaka City University
Sumiyoshi, Osaka 558
Japan

Abstract Gelation kinetics, mechanical spectra, thermal scanning rheology (TSR), and differential scanning calorimetry (DSC) in aqueous solutions of gelling polymers and colloids such as seaweed polysaccharides (agarose, carrageenans), microbial polysaccharides (gellan, curdlan), plant polysaccharides (methylcellulose), globular proteins (casein, glycinin, β-conglycinin), fibrous proteins (gelatin, fibrin), and polyvinyl alcohol, which are related to foods, cosmetics, biomedical and pharmaceutical applications, are described. Some gelation processes at a constant temperature have been treated successfully by an equation of first order kinetics or by other modified equations, and the molecular mechanism of gel formation is discussed briefly. For water-soluble polymers, the criterion of the gel or sol based on the frequency dependence of storage and loss moduli gives valuable informations. TSR and DSC are complementary, and the combination of these methods has been proved to be useful.

Key words Gelation kinetics – mechanical spectra – thermal scanning rheology – polysaccharide – protein

Introduction

Gel–sol transitions are universal phenomena influencing our everyday life: egg white changes from sol to gel when cooked; blood clots when we have a wound, if it does not we will lose our life!; sputum formation in bronchia; coagulation of proteins in cheese making or tofu making, the former as a consequence of the aggregation of milk protein (casein) in the presence of rennet, which is obtained from the lining of calves' stomachs and contains an enzyme called chymosin, whilst the latter is a result of the coagulation of soybean proteins (mainly glycinin and β-conglycinin) in the presence of coagulant such as glucono-δ-lactone or calcium sulphate; the in-mouth dissolution of coffee jelly made from gelatin or the solidification, in the refrigerator, of concentrated soup which contains meat or fish, a traditional Irish dessert blancmange made from Irish moss mixed with milk; many other important phenomena in biological and food related fields are described previously [1–5]; a thin liquid film of paint on a car surface changes into a thin solid film through sol to gel transition; gel formation in various synthetic polymers which are used as an actuator; controlled release for drug delivery; and the basis of these phenomena is described previously [6].

Many rheological studies have been carried out for food hydrocolloids which have gelling abilities because:

i) Polysaccharides and proteins act as texture modifiers controlling the rheological properties and mouthfeel;

Colloid & Polymer Science, Vol. 275, No. 12 (1997)

ii) Polysaccharides and proteins act as model substances for studying textures of foods whose mechanical and sensory properties are far more complex;
iii) Polysaccharides and proteins are themselves important ingredients of food.

During the development of science and technology of hydrocolloids, the emphasis has been laid on:

i) The optimization of food processing, conditions of preparation and storage, (looking for the best temperature, pH, ionic strength, concentration of hydrocolloids, etc).
ii) The relation between sensory evaluation and instrumental measurement.
iii) The structure–property relation. The network structure, especially, the structure of junction zones, molecular forces, hydrogen bonding, hydrophobic interaction, ionic bonds have been studied [1, 2].

Rheological techniques widely used in hydrocolloids may be classified into (i) small deformation rheology where the linearity between stress and strain is satisfied, and therefore, the methods of analysis for experimental results have been well developed, and (ii) large deformation and fracture both of which are difficult because of non-linearity and probabilistic nature. Clark and Ross-Murphy [2], Schurz [3], Nijenhuis [4] have written excellent reviews on gelling polymers mainly from the viewpoint of a rheologist, and a unique monograph by Guenet treated thermoreversible gels [5]. The application of small deformation rheology and DSC to water soluble polymers and colloids, which have not been discussed so much in the above reviews, is discussed in the present work.

Dynamic viscoelasticity

When the colloidal solution is subjected to sinusoidal shear oscillation with an angular frequency ω and an amplitude γ_0, the strain γ^* is written as $\gamma^* = \gamma_0 \exp(i\omega t)$, where $i^2 = -1$, and t is time. Then, the stress of the same frequency is induced $\tau^* = \tau_0 \exp i(\omega t + \delta)$, where τ_0 is an amplitude and δ is a phase lag. Complex shear modulus G^* is defined as $G^* = \tau^*/\gamma^* = (\tau_0/\gamma_0)\exp(i\delta) = (\tau_0/\gamma_0)(\cos\delta + i\sin\delta)$. The relation between strain and stress is shown in Fig. 1. The real and imaginary parts G' and G'' of $G^*(=G' + iG'')$ are called storage shear modulus and loss shear modulus respectively, $G' = (\tau_0/\gamma_0)\cos\delta$, $G'' = (\tau_0/\gamma_0)\sin\delta$. The storage modulus G' is proportional to the elastic energy stored in viscoelastic material in a period of oscillation, while the loss shear modulus G'' is proportional to the dissipated energy as heat in a period of oscillation. The ratio $G''/G' = \tan\delta$ is called mechanical loss tangent. The value of $\tan\delta$ tends to infinity for a purely viscous fluid, while it tends to zero for a purely elastic solid [6].

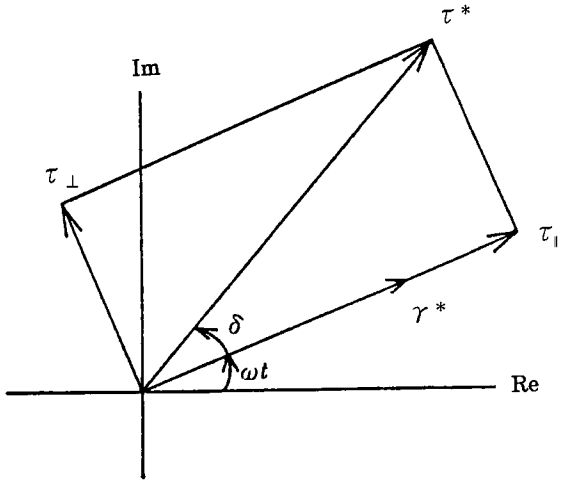

Fig. 1 Strain vector γ^* and stress vector τ^* in the complex plane. γ^* rotates with an angular velocity ω, and τ^* rotates with the same angular velocity but out of phase δ. $\tau_\parallel = \tau_0 \cos\delta$ and $\tau_\perp = \tau_0 \sin\delta$ are components of τ^* which are in-phase and out-of-phase to γ^* respectively

The oscillatory measurements are usually performed by using cone-plate or plate-plate or coaxial cylinder geometry [6]. It is necessary to cover the surface of the sample solution or dispersion by e.g. silicone oil to prevent the evaporation of water. It is also essential to use a serrated or grooved cone/plate/cylinder to avoid the slippage.

Gelation kinetics–Time dependence of storage and loss moduli G' and G'' of a solution at a constant temperature and a frequency

When a solution prepared at a non-gelling temperature is kept at a certain gelling temperature, G^* begins to increase with lapse of time. Clark and Ross-Murphy discussed the ideal condition of measurement to be adopted; the frequency and the amplitude should be as low as possible so that the structure being formed might not be broken, however, the frequency ca. 1 Hz has been chosen in most cases [2]. The geometry of the apparatus for viscoelastic measurements should be chosen so that the injected sample solution can be quenched (cooled rapidly) or can be heated rapidly. This can be satisfied generally if the required volume of sample solution is small. Generally, the gelation proceeds faster at higher temperatures for a heat-setting system whilst it proceeds faster at lower temperatures for a cold-setting system. It is easier to carry out the

rheological measurement at the temperature where the gelation proceeds slowly.

In the first order kinetics, the storage modulus is written as follows:

$$G'(t) = G'_{sat}[1 - \exp(-k(t - t_0))] , \quad (1)$$

where t_0 is the latent time (gelation time), k is the rate constant, and G'_{sat} is the saturated value of the storage modulus after a long time. Solutions of some biopolymers such as methyl cellulose [7–9], xyloglucan [10, 11], curdlan [12], glycinin and β-conglycinin [13–15] form a gel on heating, while solutions of other biopolymers such as agarose [16–18], carrageenan [19–21], gelatin [22–24] and gellan [25–30] form a gel on cooling. Therefore, the experimental procedure for the former group (gelation on heating) is as follows: after preparation of a solution at a lower temperature than the gelation temperature, the solution should be heated rapidly and kept at a higher temperature. For some polymers, it is necessary to add a coagulant to induce the gelation as in the gelation of soybean proteins and casein micelles, whilst some polymers such as methyl cellulose or xyloglucan from which some galactose residues are removed form a gel on heating without adding any coagulant.

A time evolution of G' and G'' for glycinin (11S globulin) and β-conglycinin (7S globulin), which are major gelling proteins in soybeans, in the presence of a coagulant (glucono-δ-lactone, GDL hereafter) is shown in Fig. 2 [15]. Since the quantity of the sample solution required for viscoelastic measurement was very small, ca. 0.7 ml, the temperature of the solution became almost immediately to the temperature of the measuring cell, which had been heated at 60 °C beforehand. This experiment is a simulation of tofu (soybean curd) making process. The gelation time t_0 is far shorter for glycinin than for β-conglycinin, and the gelation rate is much faster for glycinin than for β-conglycinin. The rate constant of gelation k as a function of the concentration of a coagulant GDL increased with increasing concentration of GDL for both glycinin and β-conglycinin at a fixed concentration of protein 4 wt%. The value of k as a function of protein concentration decreased with increasing concentration of protein in the presence of 0.4% GDL, which is caused by the lack of coagulant for higher concentrations of protein. When the ratio β-conglycinin/GDL was fixed to 10/1, the gelation time decreased with increasing concentration of the polymer (β-conglycinin), which is commonly observed for methyl cellulose [9], casein [31] and many other gelling polymers [2, 4].

Fig. 2 Gelation kinetics of soybean glycinin (dotted curves) and β-conglycinin (solid curves) solutions. Protein concentration, 4 wt%; glucono-δ-lactone concentration, 0.4 wt%; temperature, 60 °C; frequency, 3 Hz

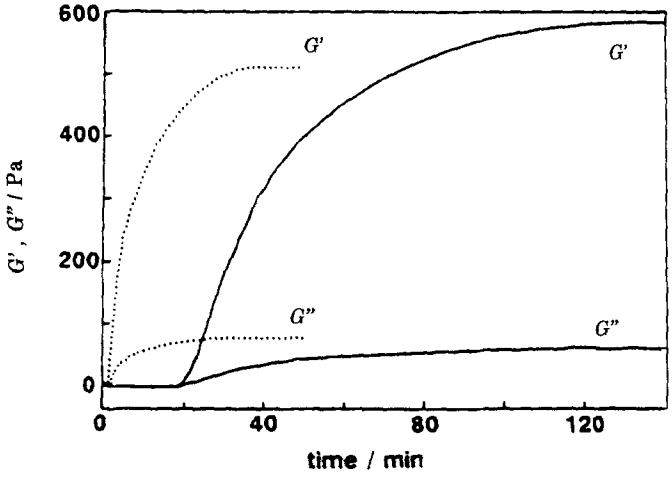

Gel formation of casein micelles in the presence of rennet has been studied extensively as a basis of cheese making process [31–36]. It is well known that κ-casein existing on the surface of casein micelles liberates hydrophilic glycomacropeptide, and the remaining hydrophobic para-casein micelles aggregate to form a three-dimensional network [31]. Niki and his coworkers [34] studied the effects of micelle size of casein on the gelation process. The increase in storage modulus as a function of time after rennet was added was again well approximated by the first order kinetics. The gelation time t_0 for small micelles was shorter than that for large micelles, and was a decreasing function of temperature. The rate constant of aggregation k was proportional to the concentration of rennet, and larger for small micelles. The final saturated value of storage modulus as a function of concentration at a constant temperature after a sufficient long time was proportional to the square of concentration, whilst it showed a maximum at 27 °C as a function of temperature at a constant concentration [34]. It is suggested that whilst hydrogen bonding is not negligible in the gelation of casein micelles, this event is governed mainly by hydrophobic interaction.

A time dependence of G' and G'' for methyl cellulose of various molecular weights is shown in Fig. 3 [9]. Since an aqueous solution of methyl cellulose shows a thermo-reversible gel–sol transition, and its behavior is the opposite to many other thermo-reversible gels which are formed on cooling and dissolved on heating, it has attracted much attention [7–9]. Solutions of higher molecular weight fractions begin to form a gel at an earlier time, and G' increases faster than solutions of lower molecular weight fractions. Although the gelation mechanism of methyl cellulose has not been clarified so well, many authors agree on the point that this polysaccharide forms a gel on heating by association induced by hydrophobic interaction [7–9]. Gelation induced from the association of polymer chains is

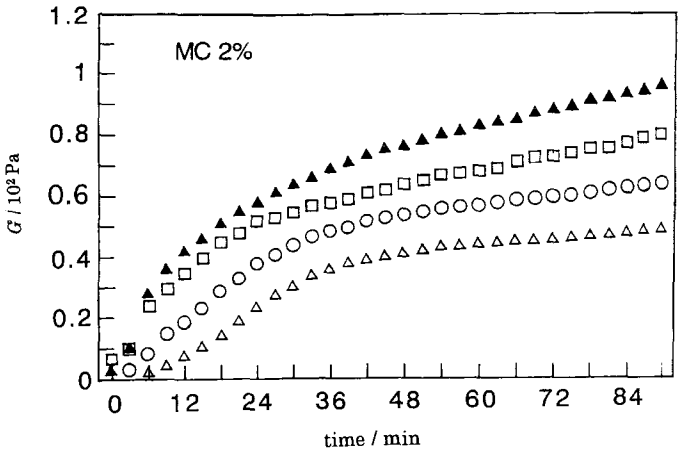

Fig. 3 Gelation kinetics of methyl cellulose of various molecular weights. Temperature, 55 °C; frequency, 3 Hz. Viscosities of each 2 wt% solution of methyl cellulose fractions are 400 cP (▲), 100 cP (□), 25 cP (○), 15 cP (△)

promoted by the increase in molecular weight of the polymer [2–5]. This has been noticed by many authors especially on the gelation of gelatin [22, 37]. The gelation mechanism of methyl cellulose will be discussed later in relation with Fig. 14.

The experimental procedure for the latter group (gelation on cooling) is as follows: after preparation of a solution at a higher temperature than the gelation temperature, the solution should be cooled rapidly and kept at a lower temperature. Figure 4 shows the gelation process of aqueous 1.95 wt% gelatin solution at various temperatures lower than the gelation temperature [24]. As is seen from this figure, storage modulus increases faster at lower temperatures than at higher temperatures. It seems that gelatin solutions do not reach an equilibrium state; storage modulus G' still increases even after 100 h.

Not all the gelation processes can be approximated well by the first order kinetics described by Eq. (1). Generally, if the gelation proceeds by two steps with different rate constants, Eq. (1) should be modified. A time evolution of dynamic modulus in blood clotting was well approximated by

$$G(t) = G_{1\mathrm{sat}}[1 - \exp(-k_1(t - t_{10}))] + G_{2\mathrm{sat}}[1 - \exp(-k_2(t - t_{20}))] , \quad (1)'$$

where k_1 and k_2 are rate constants for gelation at each step. The first process was attributed to the cross-linking reaction between fibrin fibers, and the second process was ascribed to lateral association of fibrin fibers [38, 39].

Djabourov [22] analysed the time evolution of helix content $\chi(t)$ of aqueous gelatin solution at a constant temperature by

$$\chi(t) = \chi_0[1 - \exp(-t/t_F)] + \chi_1 \log[1 + t/t_S] , \quad (1)''$$

where χ_0 and χ_1 are amplitudes of fast and slow gelation processes, and t_F and t_S are characteristic times for fast and slow processes, respectively. Axelos and Lefevbre [40] used the same Eq. (1)″ to analyze the time evolution of storage shear modulus of aqueous solutions of low methoxyl pectin in the presence of calcium ions. They found that both characteristic time t_F and t_S decreased and that χ_0 and χ_1 increased with increasing ratio of calcium/pectin.

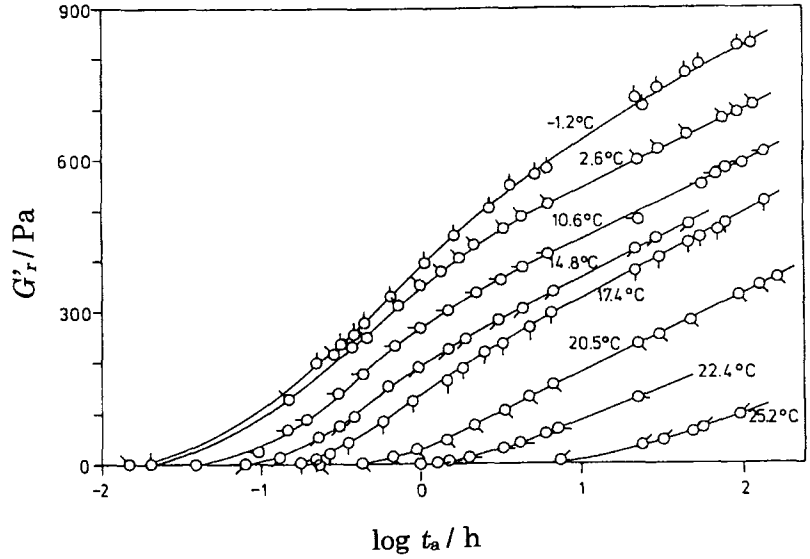

Fig. 4 Reduced storage modulus of 1.95 wt% aqueous gelatin solution as a function of ageing time at various ageing temperatures. Angular frequency, 0.39 rad/s; reference temperature, −1.2 °C. Taken from Ref. [24]

Mechanical spectra–Frequency dependence of storage and loss moduli of a solution at a constant temperature

It is well known that a power law

$$G'(\omega) \sim \omega^2, \qquad G''(\omega) \sim \omega \tag{2}$$

is valid for polymer melts at low frequencies [6(c)]. The same behavior is also found in dilute aqueous solutions of polymers. In elastic gels, both moduli show a plateau even at low frequencies [41]. The intermediate states of these two extremities are concentrated solutions in which G' and G'' show a cross-over at a certain frequency; G'' is larger than G' at lower frequencies but G' predominates G'' at higher frequencies [2,4]. Frequency dependence of G' and G'' should be observed after the accomplishment of the equilibrium at a constant temperature. It is urgent to develop an apparatus which permits the simultaneous data acquisition of G' and G'' at different frequencies, which has been realised for dielectric measurement for many years.

Frequency dependence of storage and loss moduli G' and G'' for 1–3 wt% sodium type gellan gum aqueous solutions is shown in Fig. 5 [27]. Gellan gum is a microbial polysaccharide consisting of a tetrasaccharide unit, glucose–glucuronic acid–glucose–rhamnose, and has attracted much attention because it forms a transparent, heat- and acid-resistant gels. It is believed that gellan gum molecules take double helical conformations in solutions at lower temperatures [42,43], and above a certain critical concentration, they form aggregates which play the role of junction zones, resulting in a three-dimensional network [30]. Rheological properties of aqueous gellan gum solutions are expected to change with the conformational transformation of gellan gum molecules. Since a subtle change in metal ion content will cause a drastic change in physico-chemical properties of polyelectrolyte solutions, the common sample of sodium type gellan gum was distributed to 17 laboratories with different expertises [44]. Frequency dependence of G' and G'' shown in Fig. 5 was observed at each temperature after keeping the temperature ca. 60 min to reach an equilibrium. A 1% solution of this gellan gum shows a typical dilute solution behaviour of flexible linear polymers at 0–30 °C; $G'' > G'$ for all the frequencies accessible, and both moduli increase with increasing frequency (Fig. 5A). A 2% solution also shows a dilute solution behaviour at 30 °C, but G' and G'' show a cross-over at 15 and 25 °C; $G'' > G'$ at lower frequencies but $G' > G''$ at higher frequencies (Fig. 5B). This is a so-called concentrated solution behavior. The molecular chains disentangle during a long period of oscillation at low frequencies, and the solution behaves as a viscous liquid, whilst the molecular chains do not disentangle during a short period of oscillation at high frequencies, and their entanglement points play a role of temporary knots of three-dimensional network, and as a result the solution behavior tends to that of an elastic solid. Further cooling to 0 °C leads to a weak gel behavior; $G' > G''$ at all frequencies and both moduli show only a slight frequency dependence (Fig. 5B). A 3% solution shows a concentrated solution behavior at 30 °C, however, it shows a weak gel behavior at lower temperatures < 25 °C (Fig. 5C).

It is well known that rheological properties of anionic polysaccharides such as κ-carrageenan and gellan are strongly influenced by the addition of salts [2,4]. Fig. 6 shows the mechanical spectra of 1% gellan gum solutions in the presence of sodium chloride. The cations shield the electrostatic repulsion between carboxyl groups in gellan gum molecules, and hence promote the helix formation and the association of helices. The role of cations in gelation of gellan will be discussed later in relation with Fig. 15. Storage modulus G' shows a plateau and loss shear modulus G'' shows a shallow dip at around 5×10^{-1} rad/s which has been observed for many elastic gels such as agar gels [41], bovine serum albumin gels [45], actin gels [46], β-conglycinin gels [13] (shown in the lower

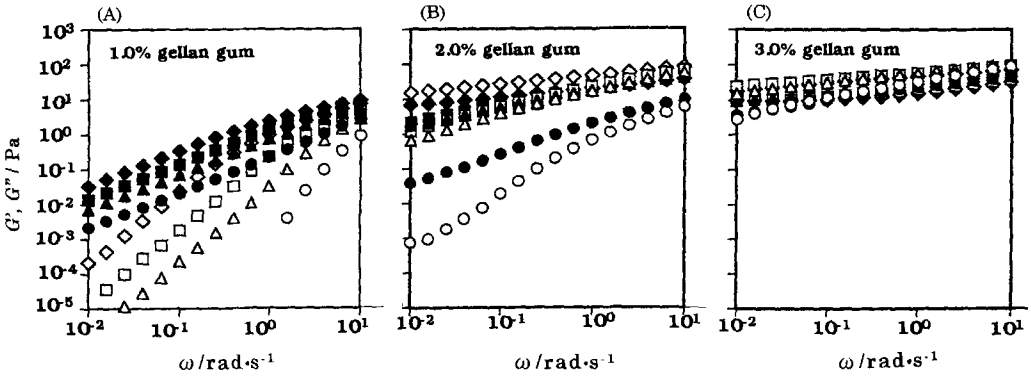

Fig. 5 Frequency dependence of G' (open symbols) and G'' (closed symbols) for 1 wt% (A), 2 wt% (B), and 3 wt% (C) gellan gum solutions at various temperatures: 0 °C (◇, ◆); 15 °C (□, ■); 25 °C (△, ▲); 30 °C (○, ●)

Colloid & Polymer Science, Vol. 275, No. 12 (1997)

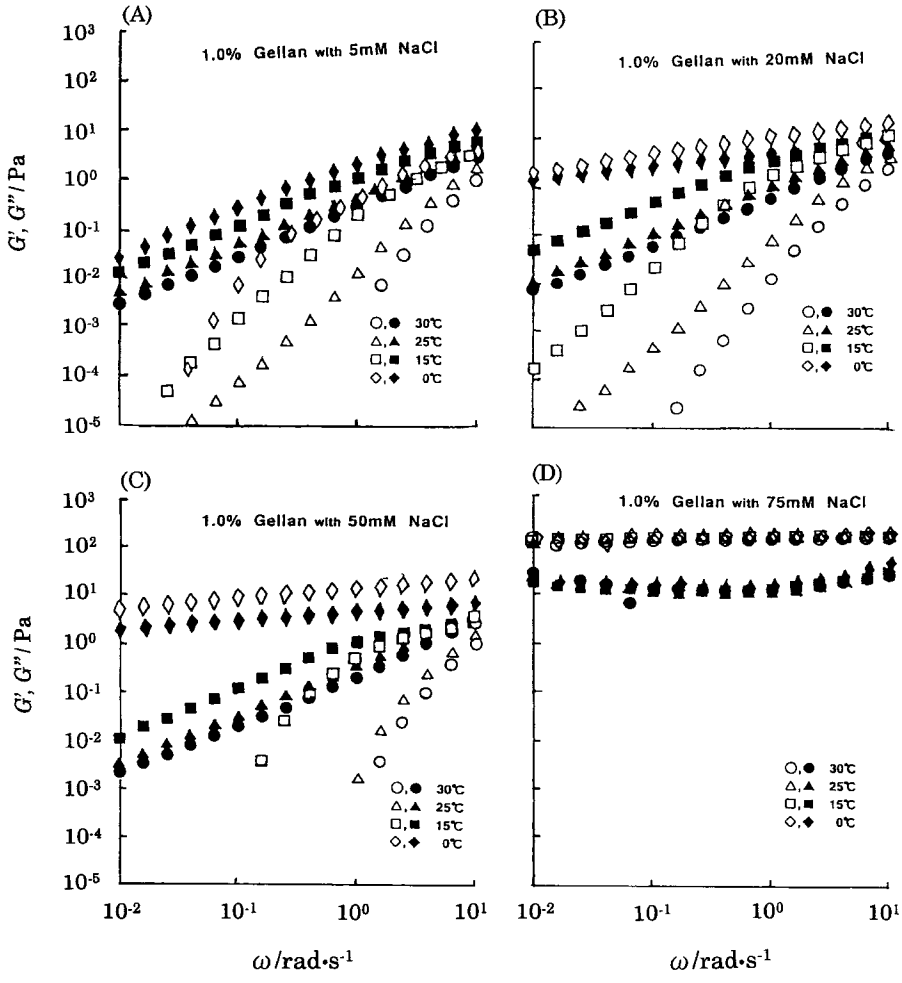

Fig. 6 Frequency dependence of G' (open symbols) and G'' (closed symbols) for 1% gellan gum solutions in the presence of sodium chloride at various temperatures: 0 °C (◇, ◆); 15 °C (□, ■); 25 °C (△, ▲); 30 °C (○, ●)

figure of Fig. 9). Some theoretical treatments have been worked out [47, 48], but the predicted dip was always too deep or too sharp, and this should be studied further. As is shown in Fig. 5A, a 1% gellan gum solution in the absence of salt behaves like a dilute solution, whilst the same solution in the presence of sodium chloride behaves like an elastic true gel.

The reason why salts enhance the gelling ability of anionic polysaccharides has been attributed to the specific binding of cations to the anionic group as proposed in a "domain model" for the gelation of carrageenan by Morris et al. [49] or/and to the electrostatic shield of repulsion of anionic groups (carboxylic groups in gellan gum molecules [28], and sulfate groups in κ-carrageenan molecules [50]) by cations in salts. Although both urea and guanidine hydrochloride are known to break hydrogen bonds, the storage modulus of κ-carrageenan gels increased by the addition of guanidine hydrochloride whilst it decreased by the addition of urea [51, 52]. Guanidinium ions play a similar role of cations such as potassium ions or calcium ions which increased the storage modulus of κ-carrageenan gels [21, 53–55]. Therefore, in the presence of small amount of guanidinium ions, the action of guanidinium ions to shield the electrostatic repulsion between anionic groups is more important than the breaking of hydrogen bonds.

Winter and Chambon proposed a method to determine the gelation point from mechanical spectra [56, 57]. According to their proposition, the gelation point is defined as a point where $G'(\omega) \sim G''(\omega) \sim \omega^n$. Although this method has been proposed using a chemical gel, Nijenhuis and Winter tried to apply this method to physical gels [58]. Recently, Hossain et al. [19] examined the applicability of this method to ι-carrageenan solutions. Figure 7 shows the mechanical spectra for 2% ι-carrageenan solutions at various temperatures from 45 °C to 59 °C. At 45 °C, both moduli G' and G'' show a plateau at low frequency region. G' and G'' became more frequency dependent with increasing temperature. They found that both G' and G'' became proportional to ω^n at $T_c = 57$ °C over the

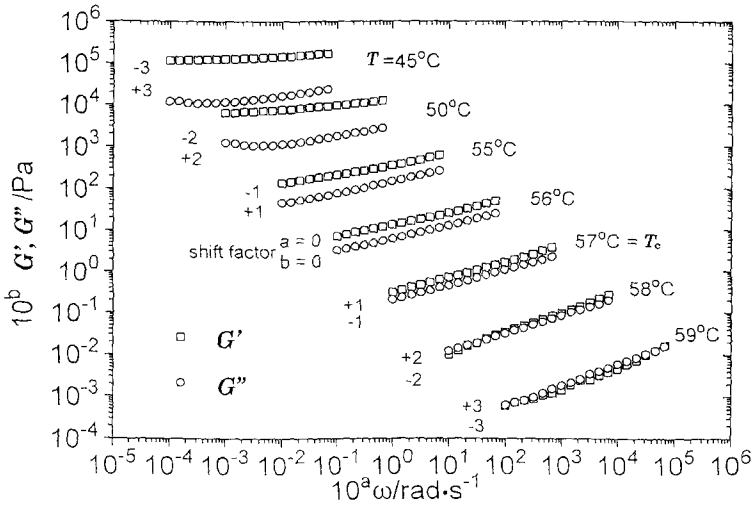

Fig. 7 Frequency dependence of G' (□) and G'' (○) for a 2 wt% ι-carrageenan solution at various temperatures. The data are shifted along both the horizontal and vertical axes by shift factors a and b, respectively to avoid the overlapping

entire angular frequency range. Further heating of the solutions gives rise to a cross-over of G' and G'', and then G'' begins to predominate G' at 59 °C. The gel point was determined as the temperature at which both G' and G'' followed the power law with the same exponent n, which was smaller than 0.5 proposed by Winter and Chambon [56, 57] or 0.8 found by Nijenhuis and Winter [58] for polyvinylchloride bis(2-ethylhexyl)phthalate systems, and the exponent was found to decrease monotonically with increasing concentration of ι-carrageenan.

Curdlan, a microbial polysaccharide consisting of β-1,3 glucan, is known to form a gel on heating, and the gel formed on heating above ca. 80 °C is thermo-irreversible and the gel formed on heating below that temperature is thermo-reversible [59, 60]. Although curdlan is not soluble in water but only can be dispersed, it is soluble in dimethylsulfoxide (DMSO). DMSO solutions of curdlan showed a similar behaviour to soluble polysaccharides as described above. The cross-over frequency of G' and G'' for DMSO solutions of curdlan shifted to lower frequencies with increasing concentration of curdlan [12] (data not shown). However, it seems difficult to prepare a high enough concentrated solution which forms a gel. Frequency dependence of storage and loss shear moduli, G' and G'', for aqueous dispersions of curdlan of 2–4% at 40 °C is shown in Fig. 8 [12]. All these dispersions showed a solid-like behaviour; $G' > G''$ at all the frequencies and shows a plateau region even at a low frequency region. Ross-Murphy et al. [61] found the similar behavior for a 0.5% xanthan aqueous solution, which was called a weak gel behavior. Similar rheological behaviors for dispersions of colloidal particles which are not soluble in water have been observed for dispersions of polystyrene lattices [62] where repulsions between colloidal particles make a so-called "colloidal crystal" [63]. It should be

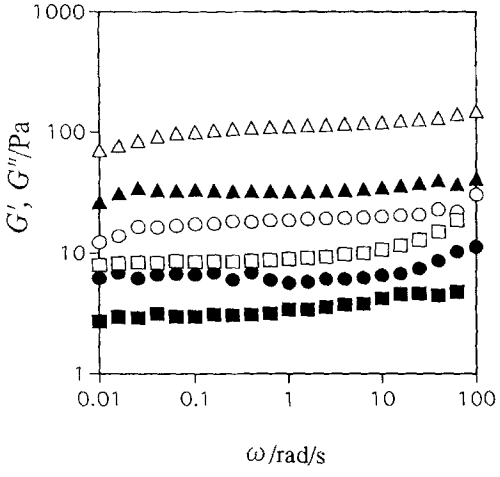

Fig. 8 Frequency dependence of G' and G'' for 2, 3, and 4 wt% aqueous dispersions of curdlan at 40 °C. (□) (G'), (■) (G''), 2 wt%; (○) (G'), (●) (G''), 3 wt%; (△) (G'), (▲) (G''), 4 wt%

noted that all these solutions or dispersions have a finite yield stress although it is not easy to determine the precise value because it depends on the sensitivity of rheological instruments.

Figure 9 shows the storage and loss moduli of 15 wt% β-conglycinin solutions which were heated at various temperatures as a function of frequency. The storage modulus G' as a function of frequency changed from a monotonical decrease with decreasing frequency to a plateau in the range from 0.0018 to 40 Hz by heating at temperatures higher than 65 °C. The increase in the storage modulus with increasing heating temperature seemed to saturate above 75 °C. Both solutions of β-conglycinin (Fig. 9) and glycinin (data not shown) showed a plateau of the storage

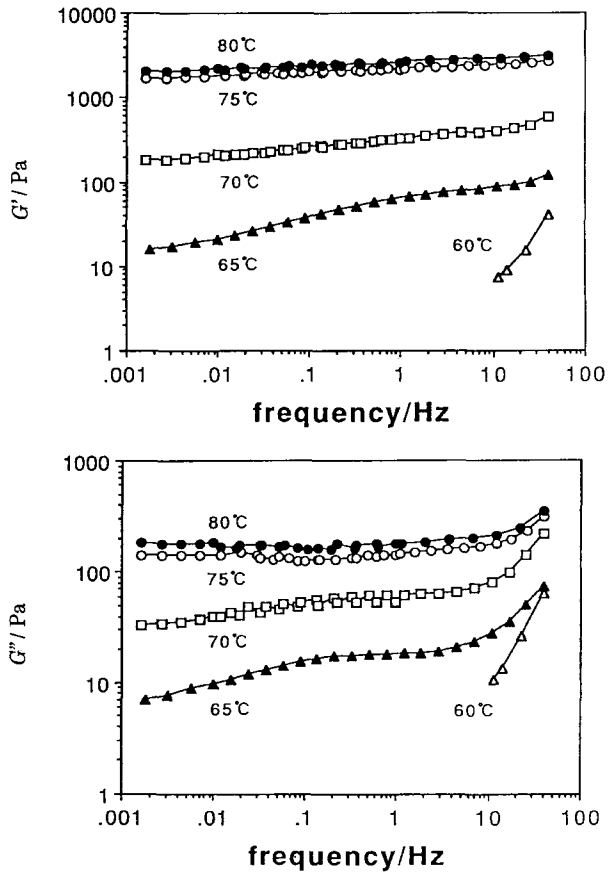

Fig. 9 Frequency dependence of G' and G'' for 15 wt% β-conglycinin solution in 35 mM phosphate buffer at pH 7.6, which had been heated at various temperatures for 30 min. (△) 60 °C; (▲) 65 °C; (□) 70 °C; (○) 75 °C; (●) 80 °C

modulus when heated at a temperature higher than 75 °C for β-conglycinin and 90 °C for glycinin. The temperature difference 15 °C is just the same to the denaturation temperature difference reported for these polymers [64, 65]. This is reasonable because the denaturation is believed to be a prerequisite for the heat-induced gelation of globular proteins [66, 67]. Absorbance change at 1618 cm^{-1} observed by FTIR (Fourier Transform Infrared Spectroscopy) as a function of temperature began to increase steeply at around 80 °C for glycinin and at around 65 °C for β-conglycinin. This was in good agreement with the above-mentioned results. The band observed at 1618 cm^{-1} in FTIR is characteristic of the β-sheet structure [68, 69]. A good correlation was found between the storage modulus at 0.87 Hz and the increase in absorption at 1618 cm^{-1}. These results suggest that heat induced gels of glycinin and β-conglycinin are formed by cross-links with intermolecular β-sheet structures [13].

Thermal scanning rheology–Temperature dependence of storage and loss moduli G' and G'' of a solution at a constant frequency

Scan rate strongly influences the results. Generally, it should be slow to be not far from equilibrium. It is recommendable to change the scan rate for unknown samples to see the effect of scan rate, and extrapolate to zero scan rate. It may be possible to analyze the scan rate dependence to understand the kinetics of the system which has not been tried so often.

Figure 10A–D shows thermal scanning rheological measurements for G' and G'' for 1.0, 2.0, 3.0 or 3.5% solution of gellan gum [30]. For lower concentrations and at higher temperatures, G'' predominates G', and a step-like increase in G'' on cooling is seen at 30 °C for a 1% gellan gum solution. The value of G' for a 1% gellan gum solution was too small to be detected by the present apparatus. The molecular ellipticity $[\theta]$ at 204 nm in circular dichroism measurements [70] is also shown in Fig. 10A together with G''. The value of $[\theta]$ stays constant above 30 °C, and shows a step-like decrease at 30 °C in the cooling process, which has been attributed to coil-to-helix transition of gellan gum molecules. The step-like change of G'' observed at the same temperature should also be attributed to coil-helix transition. For a 2% gellan gum solution, both G' and G'' could be observed even at higher temperatures. G'' shows a step-like change at ~35 °C, and G' predominates below ~7 °C. The cross-over of G' and G'' occurs below the temperature of the step-like change of G'', and at the cross-over temperature, G'' shows a step-like change. The cross-over temperature is attributed to sol–gel transition temperature T_{sg} and the sol–gel transition temperature determined in this way are shown as a function of polymer concentration in Fig. 11. When the temperature of the system is lowered from a higher temperature, helices begin to be formed at T_{ch}, and a further cooling of the system leads to a gel formation. Therefore, helix formation is a pre-requisite for a gel formation. However, a dilute solution does not form a gel even if helices are formed, because the number of helices is not sufficient to percolate to form a three-dimensional network. This situation is quite similar to that observed in gelatin solution; Djabourov et al. [22] observed the gel formation only for solutions whose helix content exceeds 7%, i.e. shear modulus begins to be detected above 7% helix content. Two transition temperatures T_{ch} and T_{sg} coincide for a concentrated gellan gum solution >3.5% because, in concentrated gellan gum solutions, as soon as helices are formed, they associate to form junction zones which play a role of knots of the three-dimensional network.

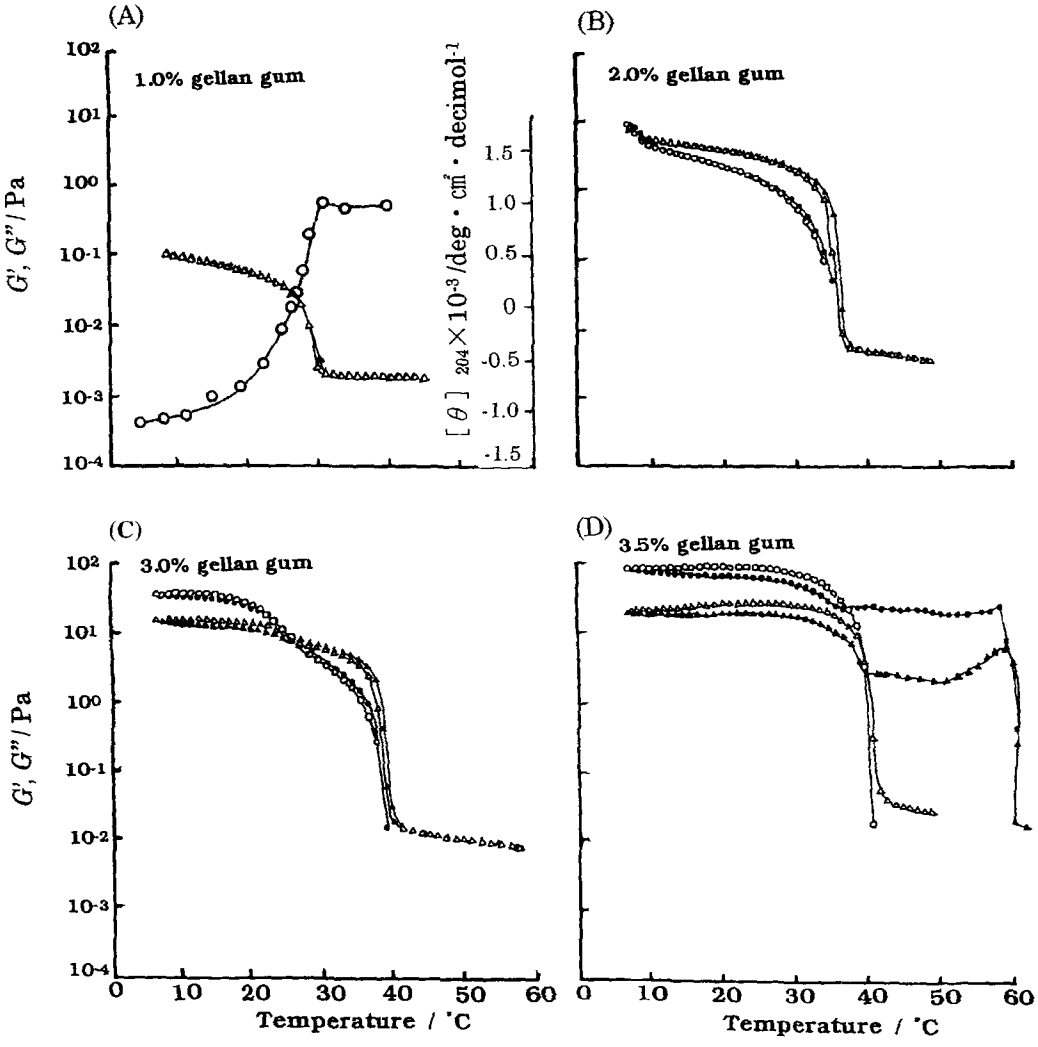

Fig. 10 Temperature dependence of G' (○, ●) and G'' (△, ▲) for gellan gum solutions of various concentrations: (A) 1.0 wt%; (B) 2.0 wt%; (C) 3.0 wt%; (D) 3.5 wt%. Open symbols are used for cooling processes and closed symbols for heating processes. Scan rate, 0.5 °C/min. Angular frequency, 0.1 rad/s. Larger open circles (◯) in (A) represent the molecular ellipticity $[\theta]$ at 204 nm for 1.0 wt% solution observed at the same scan rate. Taken from Ref. [70]

Figure 12 shows the gelation process of a 15% soybean β-conglycinin solution [14]. At a constant temperature of 80 °C, G' for the β-conglycinin solution increased, and continued to increase when the temperature was lowered from 80 °C to 20 °C at the rate of 1 °C/min. G' decreased with increasing temperature from 20 °C to 80 °C at the same rate. Values of G' are symmetrical about the vertical line $t = 3600$ s. The increase in G' after 1800 s when heating is stopped and the temperature is lowered is attributed to the further formation of network structure by hydrogen bonding which may be broken by heating from 20 °C to 80 °C. Although it is almost impossible to evaluate the contribution of hydrophobic interactions, hydrogen bonding, ionic interactions and covalent bonding quantitatively because these interactions operate simultaneously [2, 67], Fig. 12 clearly shows the important contribution of hydrogen bonding to the gel formation of β-conglycinin.

DSC study

Differential scanning calorimetry (DSC) has been used to study the gel–sol transition, the denaturation of proteins, the gelatinization of starch and the state of water in gels. The heat absorbed per unit time dQ/dt is given by $C\,dT/dt$, where C is the heat capacity, T the temperature, and t the time. In the heating DSC measurements, dT/dt is positive, and the endothermic peak is equivalent to the maximum of the heat capacity. In the cooling DSC measurement, dT/dt is negative, and the exothermic peak is again equivalent to the maximum of the heat capacity. It is generally recognized that an endothermic peak appears when the system changes from the ordered state to the disordered state such as the melting of crystals or the transition from gel to sol or gelatinization of starch, whilst an exothermic peak appears when the system changes from the disordered state to

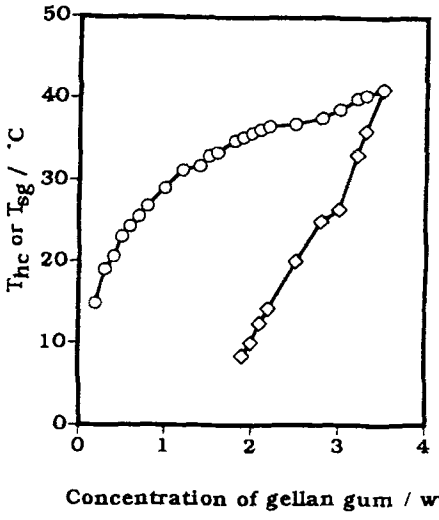

Fig. 11 Coil–helix transition temperature T_{ch} (○), and sol–gel transition T_{sg} (◇), from thermal scanning rheological measurements for gellan gum solutions in the cooling process as a function of concentration of gellan gum

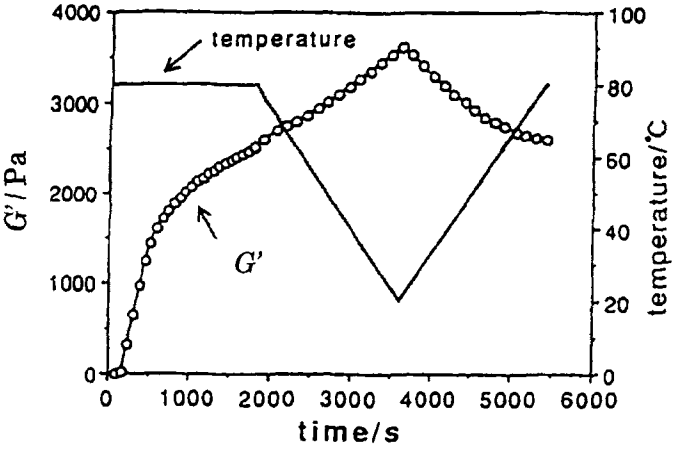

Fig. 12 Gelation process of 15% (w/v) soybean β-conglycinin solution at pH 7.6. The solution was heated at 80 °C for 30 min (= 1800 s), and then cooled to 20 °C at 2 °C/min, and heated again to 80 °C at the same rate

ordered state such as crystallization or gel formation or retrogradation of starch. The DSC pan should be hermetically sealed to avoid the leakage of water or other volatile ingredients. Scan rate should be as slow as possible to approach the equilibrium. The scan rate dependence can be analyzed by methods proposed to understand the kinetics [71].

A zipper model approach was proposed to understand the thermo-reversible gel–sol transition [72]. According to this approach, a gel is assumed to consist of zippers and each single zipper consists of N parallel links which are secondary weak bonds such as hydrogen bonds. The dis-

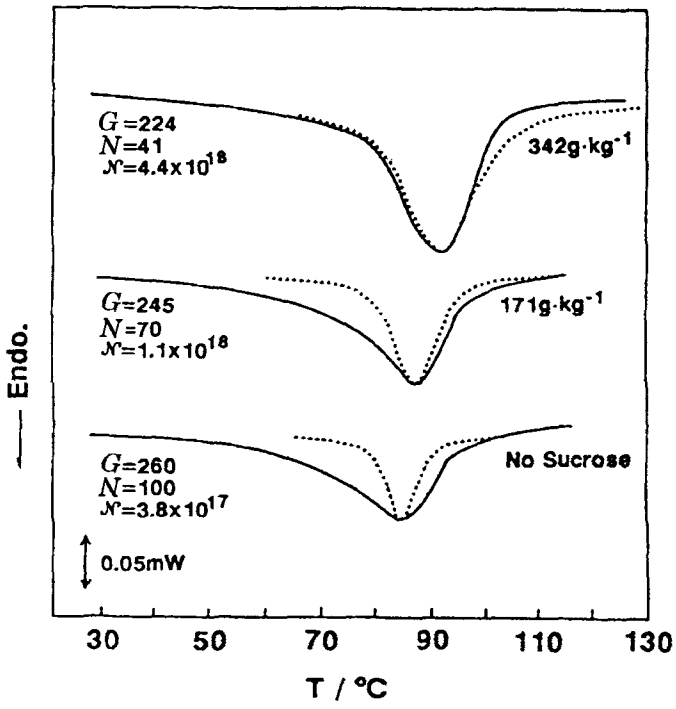

Fig. 13 Heating DSC curves of 2.0 wt% agarose gels with and without sucrose. Scan rate, 2 °C/min. Dotted curves represent the calculated curves using Eq. (3). The bonding energy is fixed as $2000k$. The number of zippers $\mathcal{N}$ per gram of a gel and the rotational freedom of links G are determined from the curve fitting, and are shown beside each curve

solution of gels can be simulated as an opening process of molecular zippers from both ends. Assuming the bonding energy ε required to open a link is the same for all the links, and that each open link can take G orientations, i.e. the open state of a link is G-fold degenerate, corresponding to the rotational freedom of a link, the heat capacity of the system can be represented by these structural parameters [72]:

$$C/k = [\ln(G/x)]^2 \{2x/(1-x)^2 + N(N+1)x^N[-x^{N+1} + (N+1)x - N]/[1-(N+1)x^N + Nx^{N+1}]^2\}, \quad (3)$$

where $x = G\exp(-\varepsilon/kT)$, and k is Boltzmann constant.

Figure 13 shows the heating DSC curves of agarose gels with and without sucrose [73]. Sucrose shifted the endothermic peak to higher temperatures, which should be attributed to one or both of the following two possibilities: (i) sucrose immobilises water molecules and the effective water content in the gel decreases with increasing sucrose concentration, so that the effective concentration of agarose increases, (ii) sucrose molecules interact directly with agarose molecules and promote the formation and aggregation of helices which play a role of knots for the

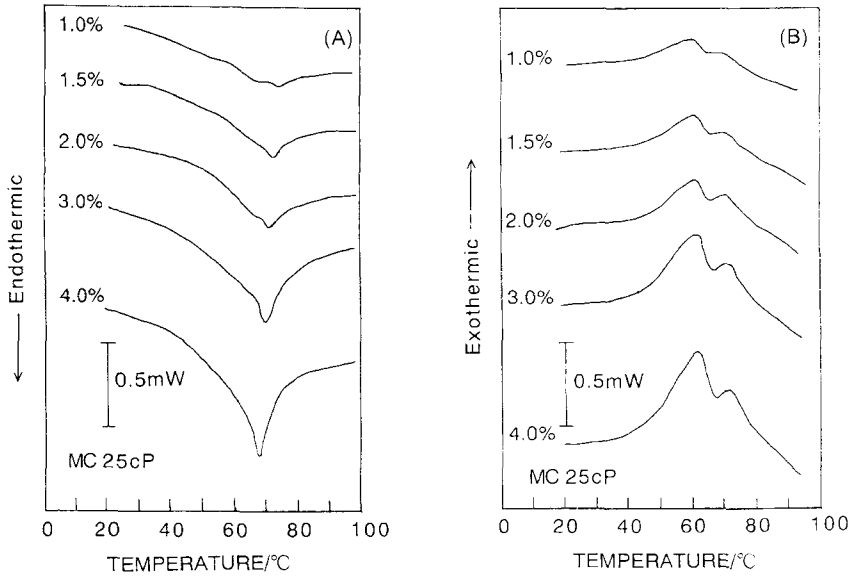

Fig. 14 Heating (A) and cooling (B) DSC curves for MC 25 cP of various concentrations. Scan rate: 1 °C/min

network formation. Assuming the number of links N which constitute a single zipper is proportional to the molecular weight of a junction zone, which is determined from a modified theory of rubber elasticity [74], the number of zippers and the rotational freedom of links were determined. From this zipper model approach, it was suggested that the number of parallel links constituting a single zipper decreases whilst the number of zippers increases with increasing concentration of sucrose; as a result, the number of elastically active chains increases but each chain becomes shorter by the addition of sucrose. Then, the molecular movement of the chains are restricted leading to the lower values of the rotational freedom.

Figure 14 shows heating DSC curves of methyl cellulose solutions of various concentrations [9]. As was shown in Fig. 3, the gelation begins to occur earlier for higher molecular weight fractions than for lower molecular weight fractions. A similar situation is also recognized for changing concentrations, i.e. the solutions of higher concentrations have a greater tendency to form a gel than those of lower concentrations, therefore, a concentrated solution showed an endothermic peak accompanying gel formation at a lower temperature than dilute solutions. The cooling DSC curves split into two peaks. Haque and Morris [7] also observed the same phenomenon, and interpreted that the gel–sol transition occurs in two steps. However, it was suggested that it could be also induced by the polydispersity of the samples according to the GPC analysis: the higher molecular weight fraction has a stronger tendency to form a gel than the lower molecular weight fractions [9], as mentioned above for Fig. 3. The apparent two step gelation process may be also induced by the gelation at a lower temperature by a higher molecular weight fraction and then followed by the gelation at a higher temperature by a lower molecular weight fraction. This should be studied immediately using monodisperse samples.

Figure 15 shows DSC heating curves of aqueous solutions of gellan gum of various concentrations [28]. An endothermic peak shifted to higher temperatures up to 3% with increasing concentration of gellan gum and it split into multiple peaks above 3.2%. The endothermic peak temperature of a 1% solution coincides with the coil–helix transition temperature which was observed by thermal scanning rheology and circular dichroism at the same scan rate (Fig. 10). The concentration of the solution above which the DSC heating curves began to split into multiple peaks coincided with that above which the remarkable thermal hysteresis began to appear [28]. The appearance of multiple endothermic peaks in heating DSC curves should be attributed to the presence of various kinds of junction zones with different thermal stabilities; this may be induced by the difference in bonding energies or/and in the degrees of rotational freedom and/or in the number of parallel links in the zipper model approach. The difference of enhancing the structural formation by monovalent and divalent cations appears clearly in cooling DSC curves which are observed from 100, 90, 80 and 70 °C (the temperature to which the solution was heated) for gellan gum solutions; the size of the exothermic peak was not influenced for solutions containing monovalent cations whilst it decreased with decreasing temperature to which the temperature was raised, indicating that the structure formed in the presence of divalent cations is far more heat resistant than that formed in the presence of monovalent cations [28]. However, this structure seems to be destroyed when the solution was heated to 110 °C, and

Colloid & Polymer Science, Vol. 275, No. 12 (1997)

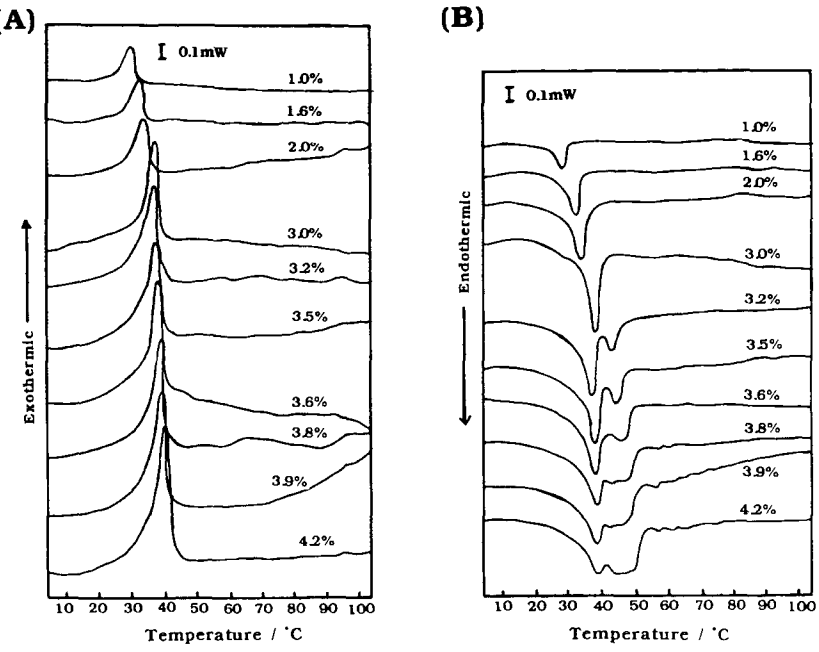

Fig. 15 Cooling (A) and heating (B) DSC curves for gellan gum solutions of various concentrations. Figures beside each curve represent the concentration of gellan gum. Cooling and heating rate: 0.5 °C/min

the possibility of the formation of ionic bonds by divalent cations may be excluded [30].

Effects of glucose on the gel–sol transition of gellan gum was examined [75]. A small amount of glucose shifted the endothermic peak temperature to lower temperatures, and further addition shifted it to higher temperatures (Fig. 16). The reason why a small amount of glucose shifted the endothermic peak temperature to lower temperatures is not clear at present. The zipper model approach was applied again to understand the effect of glucose on the gel–sol transition of gellan gum, and it was suggested that the addition of glucose increases the number of elastically active network chains, which is induced by the increase in the number of zippers, and at the same time the rotational degrees of freedom decrease because the molecular motion is hindered.

Tanaka and Nishinari recently proposed a new method to determine the structure of junction zones based on the lattice-theoretical description of network forming solutions [76]. According to this treatment, the concentration c^*, the gel–sol transition temperature T_{gs}, and the molecular weight M are related to each other by

$$\ln c^* = \zeta\varepsilon/kT - \ln M/(s-1) + \text{const.}, \qquad (4)$$

where ζ is the number of sequential units on a chain participating in a network junction, s the junction multiplicity, i.e. the number of chains combined to a single junction, k the Boltzmann constant, ε the bonding energy, i.e. the enthalpy change for binding a single repeat unit into the network junction. Figure 17 shows the plot of $\ln c^*$ against $10^3/T_{gs} + \ln M$ for poly(vinyl alcohol) (PVA)

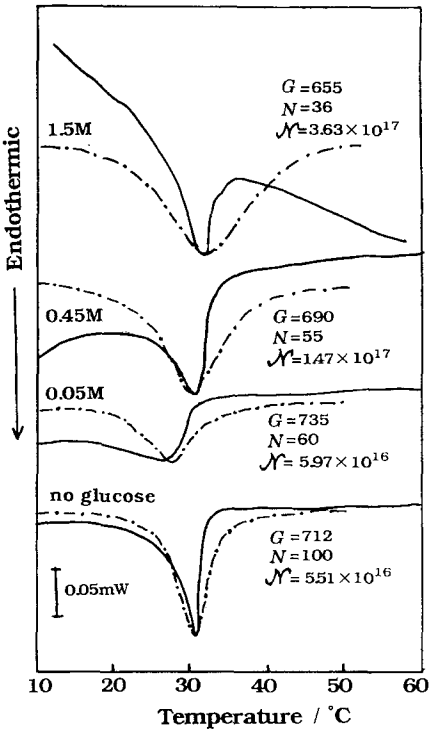

Fig. 16 Heating DSC curves of 1 wt% gellan gum solutions with and without glucose (solid curves) and the best fitted calculated curves (dot-and-line curves) using Eq. (3)

gels prepared from freeze-thaw cycles [77], where T_{gs} is taken as an endothermic peak temperature in a heating DSC curve. PVA gels prepared by freezing processes are

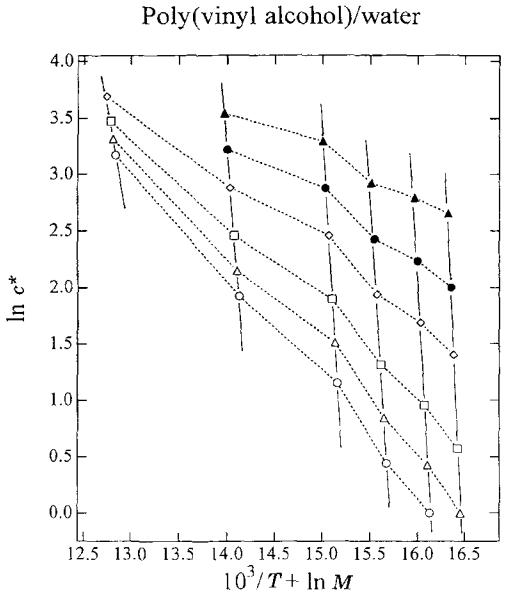

Fig. 17 Tanaka plot for PVA gels with different degrees of polymerization. Dotted transverse lines are isothermal lines connecting the following symbols: (▲) T = 364 K; (●) 360 K; (◇) 356 K; (□) 351 K; (△) 347 K; (○) 344 K. Solid longitudinal lines from left to right: DP = 470, DP = 1700, DP = 4800, DP = 8000, DP = 12 600, DP = 17 900

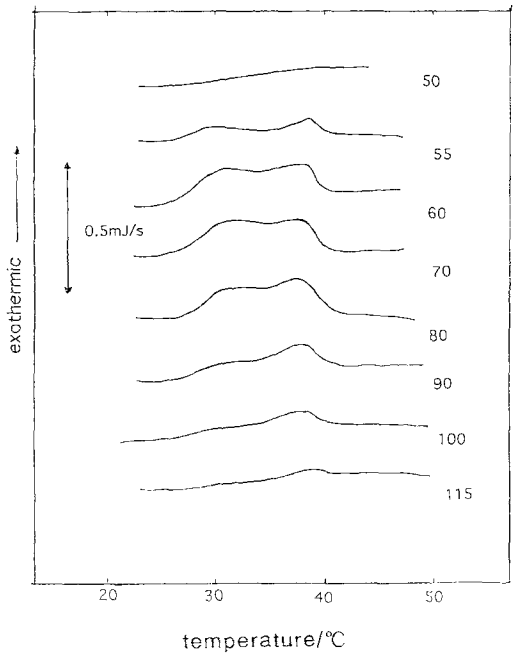

Fig. 18 Cooling DSC curves of 2 wt% curdlan aqueous dispersions kept at various temperatures for 60 min. Cooling rate, 1 °C/min. The numbers beside each curve represent the temperature in °C at which the dispersion was kept

expected to be a possible new material in the biomedical field, stimulating many investigations [78–81]. The slope $-B$ of the dotted line at constant T_{gs} gives $-1/(s-1)$, whilst the slope $-A$ of the solid line at constant M gives $\zeta = 10^3/kA/\varepsilon$. The value of $-B$ ranges from 2.0 to 3.4, whilst $-A$ is about 11.8 irrespective of molecular weight $M = 44 \times \mathrm{DP}$, where DP is the degree of polymerization. Then, the junction multiplicity s was estimated to be 2–3, and the number of sequential units along the chain ζ was 120–124 assuming that $\varepsilon = 100k$–$500k$.

Endothermic peaks appeared in heating DSC curves for curdlan dispersions, and exothermic peaks appeared in

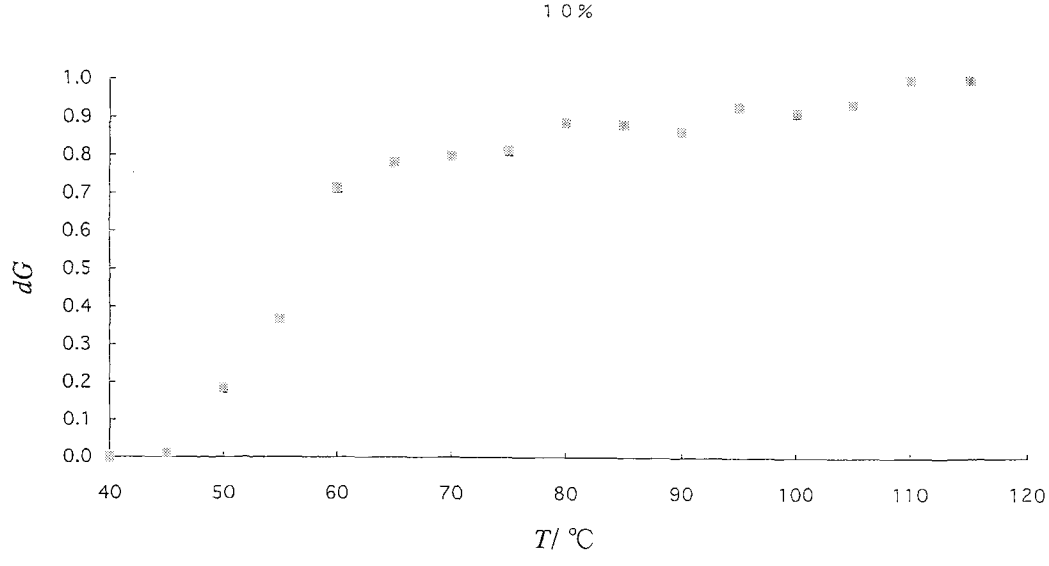

Fig. 19 The degree of thermo-irreversible gelation dG for a 10 wt% aqueous dispersion of curdlan as a function of heating temperature (see the text)

cooling DSC curves. Even after the temperature was raised above 80 °C, however, the cooling DSC curves still showed double exothermic peaks as shown in Fig. 18, which seemed contradictory to the assertion that curdlan dispersions form a thermo-irreversible gel when heated above 80 °C [59, 60]. Figure 19 shows the degree of thermo-irreversible gelation dG which is defined as

$$dG = 1 - \Delta H_{2T}/\Delta H_1 \quad (5)$$

for 10% aqueous dispersion of curdlan, where ΔH_{2T} is the endothermic enthalpy determined from the endothermic peak in the second DSC heating curve for a curdlan aqueous dispersion kept at temperature T for 60 min, and ΔH_1 is the endothermic enthalpy in the first heating curve. If gels formed by heating are completely thermo-irreversible, no endothermic peak should appear in the second DSC heating curve and in this case $dG = 1$. On the contrary, if gels are completely thermo-reversible the second run heating DSC curve will give exactly the same endothermic enthalpy, and then $dG = 0$. How fast dG increases with increasing heating temperature should depend on molecular weight and concentration of curdlan, and this should be explored in the future.

References

1. Nishinari K, Yano T (eds) (1990) Science of Food Hydrocolloids. Asakura Shoten, Tokyo
2. Clark AH, Ross-Murphy SB (1987) Adv Polym. Sci. 83:57
3. Schurz J (1991) Prog Polym Sci 16:1
4. Te Nijenhuis K (1997) Adv Polym Sci 130:1
5. Guenet J-M (1992) Thermoreversible Gelation of Polymers and Biopolymers. Academic Press, London
6. (a) Ferry JD (1980) Viscoelastic Properties of Polymers, 3rd ed. Wiley, New York; (b) Sperling LH (1992) Introduction to Physical Polymer Science, 2nd ed. Wiley, New York; (c) Strobl G (1996) The Physics of Polymers. Springer, Berlin
7. Haque A, Morris ER (1992) Carbohydr Polym 22:161
8. Vigouret M, Rinaudo M, Desbrieres JJ (1996) J Chim Phys 93:858
9. Nishinari K, Hofmann KE, Moritaka H, Kohyama K, Nishinari N (1997) Macromol Chem Phys 198:1217
10. Reid JSG, Edwards M, Dea ICM (1988) In: Phillips GO, Wedlock DJ, Williams PA (eds) Gums and Stabilisers for the Food Industry, Vol. 4. IRL Press, Oxford, p 391
11. Shirakawa M, Yamatoya K, Nishinari K, Food Hydrocoll, in press
12. Hirashima M, Takaya T, Nishinari K, Thermochim Acta, in press
13. Nagano T, Akasaka T, Nishinari K (1994) Biopolymers 34:1303
14. Nagano T, Mori H, Nishinari K (1994) J Agric Food Chem 42:1415
15. Kohyama K, Nishinari K (1993) J Agric Food Chem 41:8
16. Matsuhashi T (1990) In: Harris P (ed) Food Gels, Elsevier, Amsterdam
17. Nishinari K, Watase M, Kohyama K, Nishinari N, Koide S, Ogino K, Oakenfull O, Williams PA, Phillips GO (1992) Polymer J 24:871
18. Tokita M, Hikichi K (1987) Phys Rev A 35:4329
19. Hossain KS, Nemoto N, Nishinari K, Nihon Reoroji Gakkaishi, in press
20. Nishinari K, Watase M (1992) Thermochim Acta 206:149
21. Richardson RK, Goycoolea FM (1994) Carbohydr Polym 24:223
22. Djabourov M, Leblond J, Papon P (1988) J Phys France 49:319
23. Carvalho W, Djabourov M, In: The Wiley Polymer Networks Group Review, number 1, in press
24. Te Nijenhuis K (1981) Colloid Polym Sci 259:522
25. Robinson G, Manning CE, Morris ER (1991) In: Dickinson E (ed.) Food polymers, gels and colloids, The Royal Society of Chemistry, Cambridge, p 22
26. Moritaka H, Nishinari K, Taki M, Fukuba H (1995) J Agric Food Chem 43:1685
27. Miyoshi E, Takaya T, Nishinari K (1995) Macromol Symp 99:83
28. Miyoshi E, Takaya T, Nishinari K (1994) Food Hydrocoll 8:505, 529
29. Miyoshi E, Takaya T, Nishinari K (1996) Carbohydr Polym 30:109
30. Miyoshi E, Takaya T, Nishinari K (1995) Thermochim Acta 267:269
31. Niki R, Sasaki T (1987) Jpn J Zootech Sci 58:1032
32. Brinkhuis J, Payens TA (1984) Biophys Chem 19:75
33. de Kruif KG, Hoffmann AM, van Marle ME, van Mil PJJM, Roefs SPFM, Verheul M, Zoon N (1996) Faraday Discuss 101:185
34. Niki R, Kohyama K, Sano Y, Nishinari K (1994) Polym Gels Netw 2:105
35. Zoon P, van Vliet T, Walstra P (1989) Neth Milk Dairy J 43:35
36. Tokita M, Hikichi K, Niki R, Arima S (1982) Biorheology 19:695
37. Busnel JP, Clegg SM, Morris ER (1988) In: Phillips GO, Wedlock DJ, Williams PA (eds) Gums and Stabilisers for the Food Industry, Vol. 4, IRL Press, Oxford, p 105
38. Fukada E, Kaibara M (1973) Biorheology 10:129
39. Kaibara M (1996) Biorheology 33:101
40. Axelos MAV, Lefevbre J (1989) Abstract book of 24th Symposium of French Group of Rheology
41. Nishinari K (1976) Jpn J Appl Phys 15:1263
42. Dentini M, Coviello T, Burchard W, Crescenzi V (1988) Macromolecules 21:3312
43. Shi X, Milas M, Rinaudo M (1990) Biopolymers 30:451
44. Nishinari K (1996) Carbohydr Polym 30:75
45. Richardson RK, Ross-Murphy SB (1981) Br Polym J 13:11
46. Zaner KS, Stossel TP (1983) J Biol Chem 258:11004
47. Marvin RS, Oser H (1963) J Res Nat Bur Stand (USA) 67B 87
48. Chompff AJ, Prins W (1968) J Chem Phys 48:235
49. Morris ER, Rees DA, Robinson G (1980) J Mol Biol 138:349
50. Watase M, Nishinari K (1982) Rheol Acta 21:318
51. Nishinari K, Watase M, Williams PA, Phillips GO (1990) J Agric Food Chem 38:1188
52. Watase M, Nishinari K (1986) Food Hydrocoll 1:25
53. Morris VJ, Chilvers GR (1983) Carbohydr Polym 3:129
54. Morris VJ, Belton PS (1980) J Chem Soc Chem Comm 983
55. Watase M, Nishinari, K (1982) Colloid Polym Sci 260:971
56. Winter HH, Chambon F (1986) J Rheol 30:367
57. Chambon F, Winter HH (1986) J Rheol 30:683
58. Te Nijenhuis K, Winter HH (1989) Macromolecules 22:411

59. Miwa M, Nakao Y, Nara K (1994) In: Nishinari K, Doi E (eds) Food Hydrocolloids: Structures, Properties and Functions, Plenum Press, New York p 119
60. Harada T, Okuyama K, Konno A, Koreeda A, Harada A (1994) Carbohydr Polym 24:101
61. Ross-Murphy SB, Morris VJ, Morris ER (1983) Faraday Symp Chem Soc 18:115
62. Matsumoto T, Okubo T (1991) J Rheol 35:135
63. Kose A, Ozaki M, Takano K, Kobayashi Y, Hachisu S (1973) J Colloid Interface Sci 44:330
64. Damodaran S (1988) J Agric Food Chem 36:262
65. Hermansson A-M (1986) J Am Oil Chem Soc 63:658
66. Doi E (1993) Trends Food Sci Technol 4:1
67. Clark AH, Lee-Tuffnell CD (1986) In: Mitchell JR, Ledward DA (eds) Functional Properties of Food Macromolecules, Elsevier Appl. Sci. Publ., London, p. 203
68. Surewicz WK, Mantsch MM, Chapman D (1993) Biochemistry 32:389
69. Susi H, Byler DM (1987) Arch Biochem Biophys 258:465
70. Tanaka Y, Sakurai M, Nakamura K, (1996) Food Hydrocoll 10:133
71. Hatakeyama T, Quinn FX (1994) Thermal Analysis – Fundamentals and Application to Polymer Science. Chichester, UK
72. Nishinari K, Koide S, Williams PA, Phillips GO (1990) J Phys France 51:1759
73. Nishinari K, Watase M, Kohyama K, Nishinari N, Oakenfull D, Koide S, Ogino K, Williams PA, Phillips GO (1992) Rep Prog Polym Phys Japan 35:169
74. Oakenfull D (1984) J Food Sci 49:1103
75. Miyoshi E, Takaya T, Nishinari K, Polym Gels Netw, in press
76. Tanaka F, Nishinari K (1996) Macromolecules 29:3625
77. Nishinari K, Watase M, Tanaka F (1996) J Chim Phys 93:880
78. Watase M, Nishinari K (1988) Makromol Chem 189:871
79. Kanaya T, Ohkura M, Takeshita H, Kaji K, Furusaka M, Yamaoka H, Wignall GD, (1995) Macromolecules 28:3168
80. Lozinsky VI, Zubov AL, Kulakova VK, Titova EF, Rogozhin SV (1992) J Appl Polym Sci 44:1423
81. Takigawa T, Kashihara H, Urayama K, Masuda T (1992) Polymer 33:2334